ALL-DIGITAL IMPULSE RADIO FOR MUI/ISI-RESILIENT MULTI-USER COMMUNICATIONS OVER FREQUENCY-SELECTIVE MULTIPATH CHANNELS

Christophe J. Le Martret [1] *and Georgios B. Giannakis* [2]

[1] DGA/CELAR, France. Currently visiting researcher with the ECE Dept., Univ. of Minnesota, Minneapolis, MN

[2] ECE Dept., Univ. of Minnesota, Minneapolis, MN

{lemartre,georgios}@ece.umn.edu

ABSTRACT

Impulse radio (IR) is an ultra-wideband system with attractive features for baseband asynchronous multiple access (MA), multimedia services, and tactical wireless communications. Implemented with analog components, the continuous-time IRMA model utilizes pulse-position modulation (PPM) and random time-hopping codes to alleviate multipath effects and suppress multiuser interference (MUI). We introduce a novel continuous-time Multiple Input Multiple Output (MIMO) PPM-IRMA scheme, and derive its discrete-time equivalent model. Relying on a time-division-duplex access protocol and orthogonal user codes, we design composite linear and non-linear receivers for the downlink. The linear step eliminates MUI deterministically and accounts for frequency-selective multipath, while a Maximum Likelihood (ML) receiver performs symbol detection.

1. INTRODUCTION

The idea of transmitting digital information using ultra-short impulses was first presented in [10] and called *Impulse Radio*. It relies on PPM and time diversity that is gained by repeating the same symbol many (≥ 1000) times according to a random code. The attractive features of IR can be summarized as follows: it transmits at baseband; thus, neither intermediate frequency nor carrier synchronization processing is needed; it consumes minimal power; and, it is robust against jamming and multipath. IR has also been extended to multi-user communications in [5] where it is known as impulse radio multiple access (IRMA). Its principle is based on asynchronous transmissions between users and statistical MUI cancellation relying on power control.

Subsequent works have focused on optimizing the efficiency of IRMA by characterizing the channel [9], improving the modulation format [4], and addressing networking aspects [1]. An application of the conventional IRMA has been considered in [7] for the radio link in a multimedia PCS communication scenario.

In all IRMA schemes proposed so far, the multiuser interference is randomized and only statistically suppressed provided that (strict) power control is successfully applied. This solution may be well motivated for ad hoc architectures but prevents one from taking advantage of multiuser detection (MUD). Indeed, the latter brings benefits over statistical MUI cancellation when the number of users is small and thus the independent Gaussian approximation of the interference is no longer valid. Moreover, in their digital implementation MUD receivers facilitate channel equalization to mitigate propagation effects. And finally, MUD alleviates the need for power control.

We recently presented in [3] a new continuous-time modeling approach for the PPM-IRMA and derived an approximate model which turns out to be Single Input Single Output (SISO). We present here the exact model which is multiple input multiple output (MIMO). This model is realizable by a set of parallel linear modulators at the transmitter and a set of parallel matched filters at the receiver (Section 3). The input to the linear modulators can be expressed as the output of a filterbank, fed by a non-linear transformation of the symbols.

Relying on the time-division multiplex IRMA protocol and the orthogonal codes designed in [2] for multi-user communications in wireless cellular systems, we further propose digital receivers for the downlink. They are composed of a linear filter for channel mitigation and user separation, followed by an ML detector for symbol recovery (Section 4).

Finally, we present performance of the different receivers (Section 5). We first simulate the performance for the three receivers in a frequency-selective multipath channel. Then we derive an upper bound on the symbol error rate (SER) for the zero forcing receiver and compare it to our simulated performance.

2. CONTINUOUS-TIME PPM-IRMA

To introduce notation and facilitate the transition from the original continuous-time PPM to the MIMO model, we first review the conventional PPM-IRMA and the novel model presented in [3] in the single-user case.

2.1. Conventional PPM-IRMA Modeling

In PPM-IRMA, each user (say the m-th) transmits each information symbol $s_m(q)$ drawn from the alphabet $\{0, 1, \ldots, A-1\}$ repeatedly over N_f frames each of duration T_f. Specifically, letting the frame index to be $k = qN_f + r$, $r \in [0, N_f - 1]$ and with $\lfloor x \rfloor$ denoting integer-floor, the q-th symbol can be written as: $s_m(q) = s_m(\lfloor k/N_f \rfloor)$. The same signal $s_m(\lfloor k/N_f \rfloor)$ is transmitted N_f times using a position-hopping sequence $\tilde{c}_m(k)$ having N_c possible hops (chips) per frame. With T_c denoting

0-7803-6521-6/00/$10.00 (c) IEEE

chip duration, we thus have $T_f = N_c T_c + T_g$, where T_g is a guard time introduced to account for processing delay at the receiver between two successive received frames (see *e.g.*, [7]). For the k-th frame and depending on the value $n_c \in [0, N_c - 1]$ of the code $\tilde{c}_m(k) = n_c$, the chip-pulse (also known as the monocycle) $w(t)$, is positioned at the n_c-th chip interval. Within this chip interval, the monocycle is shifted by $\tau_{s_m(q)}$ to implement the PPM. With these notational conventions, the m-th user's transmitted waveform is given by (see *e.g.*, [4]):

$$v_m(t) = \mathcal{P} \sum_{k=-\infty}^{+\infty} w(t - kT_f - \tilde{c}_m(k)T_c - \tau_{s_m(\lfloor \frac{k}{N_f} \rfloor)}), \quad (1)$$

where $\mathcal{P}$ is the amplitude which controls the transmitted power. The code $c_m(k)$ is a periodic pseudo-random sequence [5] with period $P_{\tilde{c}}$. We will restrict this period to be an integer multiple of the number of frames, *i.e.*, $P_{\tilde{c}} = KN_f$. Such a *block-periodic* code that will be adopted henceforth, implies a block spreading operation where each block of K information bearing symbols $\{s_m(qK), s_m(qK+1), \ldots, s_m((q+1)K-1)\}$ is spread by the same hopping sequence over KN_f frames. The parameter K can be easily adjusted and turns out to be the number of transmit symbols per burst in the TDD protocol proposed in [2].

2.2. Novel PPM-IRMA Modeling

It has been shown in [3] that (1) can be re-expressed as:

$$v_m(t) = \mathcal{P} \sum_{a=0}^{A-1} v_{m,a}(t) \quad (2)$$

where each $v_{m,a}(t)$ is a linear modulator given by:

$$v_{m,a}(t) = \sum_{n=-\infty}^{+\infty} u_{m,a}(n) w_a(t - nT_c), \quad (3)$$

with $w_a(t) := w(t - \tau_a)$. Sequence $u_{m,a}(n)$ is deduced from the symbols and the hopping sequence by

$$u_{m,a}(n) := \beta_a(s_m(\lfloor n/(N_c N_f) \rfloor)) c_m(n), \quad (4)$$

where $\beta_a(\cdot)$ is a non-linear function defined by:

$$\text{for } s, a \in [0, A-1], \quad \beta_a(s) := \begin{cases} 1 & \text{if} \quad s = a, \\ 0 & \text{otherwise}, \end{cases} \quad (5)$$

and where $c_m(n)$ is deduced from $\tilde{c}_m(n)$ as:

$$c_m(n) = \begin{cases} 1 \text{ if } \quad \tilde{c}_m(\lfloor n/N_c \rfloor) = n - \lfloor n/N_c \rfloor N_c, \\ 0 \text{ otherwise.} \end{cases} \quad (6)$$

Moreover, (4) can be implemented with a discrete-time filterbank as shown in Fig. 1 where $c_{m,k}(p)$ is defined as:

$$c_{m,k}(p) = \begin{cases} c_m(p), & \text{for } kN_f N_c \le p \le (k+1)N_f N_c - 1, \\ 0 & \text{otherwise.} \end{cases}$$

Hence, the continuous-time PPM-IRMA transmission with block-periodic codes can be depicted as in Fig. 2, where the notation $F(K, N_1, c_m)$ stands for the filterbank precoder of Fig. 1.

Unlike the conventional model, we have assumed here for simplicity that $T_g = 0$. In fact, our novel model encompasses the case $T_g \neq 0$ as well, by setting $T_g = N_g T_c$, with N_g integer and restricting the sequence $\tilde{c}_m(n)$ to take its values in $[0, N_c' - 1]$ where $N_c' := N_c - N_g$. For the rest of the paper, we will assume that $T_g = 0$.

This novel model can be approximated (see [3]) by moving the continuous delays τ_a into the modulating sequence $u_{m,a}(n)$ which increases the symbol rate of the linear modulators in (3). This leads to a SISO discrete-time equivalent model involving one transmit filter and one receive filter along with a sampling rate greater than $1/T_c$.

We present next the exact discrete-time equivalent model for the novel PPM-IRMA representation which is MIMO.

3. THE DISCRETE-TIME MIMO MODEL

The transmitted symbols are sent at a rate $1/T_c$, and we sample the received signal at the same rate. Adhering to PPM, this can only be achieved by passing the received signal through A parallel filters matched to the pulses $w_a(t)$ prior to sampling. We thus arrive at the MIMO continuous-time PPM-IRMA transmission model shown in Fig. 3 in the single-user case where $h_m(t)$ is the propagation channel impulse response.

It follows from (2) and (3) that the chip-sampled matched filter output of the b-th branch at the receiver is:

$$y_{m,b}(n) = \mathcal{P} \sum_{a=0}^{A-1} \sum_{k=-\infty}^{+\infty} u_{m,a}(k) h_{m,b,a}(n-k) + \eta_b(n)$$

with $h_{m,b,a}(n) := w_a(t) \star h_m(t) \star w_b(-t)|_{t=nT_c}$, and $\eta_b(n) := \eta(t) \star w_b(-t)|_{t=nT_c}$ where $\star$ stands, for convolution.

Casting (4) into a matrix form, we can express the i-th transmitted block of the a-th branch $u_{m,a}(i;p)$ of length N_1 by the $N_1 \times 1$ vector $\mathbf{u}_{m,a}(i) = \mathbf{C}_m \beta_a(\mathbf{s}_m(i))$, where $\mathbf{s}_m(i) := [s_m(iK), \ldots, s_m((i+1)K-1)]^T$ is the $K \times 1$ vector representing the symbol block of length K with the following notational convention: $\beta_a(\mathbf{s}_m(i)) := [\beta_a(s_m(iK)), \ldots, \beta_a(s_m((i+1)K-1))]^T$, and $\mathbf{C}_m := [\mathbf{c}_{m,0} \cdots \mathbf{c}_{m,K-1}]$ denotes the $N_1 \times K$ code matrix of user m with k-th column $\mathbf{c}_{m,k} := [c_{m,k}(0), \ldots, c_{m,k}(N_1 - 1)]^T$.

At the m-th receiver, according to the TDD-IRMA protocol in [2], it suffices to collect the first $N_{L_1} := N_1 + L_1$ samples per transmitted burst to enable symbol recovery. Parameter L_1 depends on the propagation channel length and the asynchronism between users. Let L denote the number of samples between two transmitted bursts. Then, the i-th $N_{L_1} \times 1$ received block corresponding to the b-th branch, defined as $\mathbf{y}_{m,b}(i) := [y_{m,b}(iL), \ldots, y_{m,b}(iL + N_{L_1} - 1)]^T$, can be expressed as:

$$\mathbf{y}_{m,b}(i) = \mathcal{P} \sum_{a=0}^{A-1} \mathbf{H}_{m,a,b} \mathbf{u}_{m,a}(i) + \boldsymbol{\eta}_b(i) \quad (7)$$

where $\boldsymbol{\eta}_b(i) := [\eta_b(iL), \ldots, \eta_b(iL+N_{L_1}-1)]^T$ and $\mathbf{H}_{m,a,b}$ are $N_{L_1} \times N_1$ Toeplitz convolution matrices given by:

$$\mathbf{H}_{m,b,a} = \begin{pmatrix} h_{m,a,b}(0) & \cdots & 0 \\ \vdots & \ddots & \vdots \\ h_{m,b,a}(L) & & h_{m,b,a}(0) \\ \vdots & \ddots & \vdots \\ 0 & \cdots & h_{m,b,a}(L) \end{pmatrix}. \quad (8)$$

We can re-express (7) for $b = 0, \ldots, A-1$ by defining the $N_{L_1}A \times 1$ vectors $\mathbf{y}_m(i) := [\mathbf{y}_{m,0}^T, \ldots, \mathbf{y}_{m,A-1}^T]^T$ which leads to:

$$\mathbf{y}_m(i) = \mathcal{P}\ \mathbf{H}_m \mathbf{u}_m(i) + \boldsymbol{\eta}(i), \quad (9)$$

where $\mathbf{u}_m(i) := [\mathbf{u}_{m,0}^T, \ldots, \mathbf{u}_{m,A-1}^T]^T$, $\boldsymbol{\eta}(i) := [\boldsymbol{\eta}_0^T(i), \ldots, \boldsymbol{\eta}_{A-1}^T(i)]^T$, and $\mathbf{H}_m$ is a block $N_{L_1}A \times N_1 A$ matrix given by:

$$\mathbf{H}_m := \begin{pmatrix} \mathbf{H}_{m,0,0} & \mathbf{H}_{m,0,1} & \cdots & \mathbf{H}_{m,0,A-1} \\ \mathbf{H}_{m,1,0} & \mathbf{H}_{m,1,1} & \cdots & \mathbf{H}_{m,1,A-1} \\ \vdots & \vdots & \ddots & \vdots \\ \mathbf{H}_{m,A-1,0} & \mathbf{H}_{m,A-1,1} & \cdots & \mathbf{H}_{m,A-1,A-1} \end{pmatrix}. \quad (10)$$

4. DIGITAL RECEIVERS FOR THE DOWNLINK

We describe here three linear receivers for the downlink of a cellular multiuser scheme, using the time division duplex and the orthogonal code design described in [2]. We assume that the known channel is time-invariant but adaptive variants of these receivers or successive interference cancellers can be also derived to handle slowly-varying channels. Although not considered here, non-linear receivers such as DFEs (see *e.g.*, [6]) are also applicable.

Because PPM is a non-linear modulation, the receivers will operate in two stages: 1) a linear filtering stage to eliminate channel effects and separate the users; and, 2) a non-linear processing stage to recover the symbols.

The i-th transmit symbol block for the downlink is given by: $\mathbf{u}(i) = \sum_{\mu=0}^{N_c-1} \mathbf{u}_\mu(i)$, while the received block at the m-th receiver is:

$$\mathbf{y}_m(i) = \mathcal{P}\ \mathbf{H}_m \mathbf{u}(i) + \boldsymbol{\eta}(i). \quad (11)$$

Based on the vector model (11), a multichannel FIR receiver can be described by a matrix $\mathbf{G}_m$ of dimension $KA \times N_{L_1}A$ as follows:

$$\widehat{\boldsymbol{\beta}}_{\mathbf{s}_m(i)} = \mathbf{G}_m \mathbf{y}_m(i) = \mathcal{P}\ \mathbf{G}_m \mathbf{H}_m \mathbf{u}(i) + \breve{\boldsymbol{\eta}}(i), \quad (12)$$

where $\widehat{\boldsymbol{\beta}}_{\mathbf{s}_m(i)} := [\widehat{\beta}_0^T(\mathbf{s}_m(i)), \ldots, \widehat{\beta}_{A-1}^T(\mathbf{s}_m(i))]^T$ is the $KA \times 1$ estimated vector of the symbols transformed by the non-linear function $\beta(\cdot)$, and $\breve{\boldsymbol{\eta}}(i) := \mathbf{G}_m \boldsymbol{\eta}(i)$ is the filtered noise.

Depending on how we select $\mathbf{G}_m$, we obtain different *linear receivers* and possible choices include: Zero Forcing (ZF), Matched Filter (MF), and Minimum Mean Square Error (MMSE). These receivers are given by:

- ZF (a.k.a. Decorrelating) Receiver

$$\mathbf{G}_m^{\mathrm{ZF}} := \mathrm{diag}\left(\mathbf{C}_m^T, \ldots, \mathbf{C}_m^T\right) \left(\mathbf{H}_m^T \mathbf{H}_m\right)^{-1} \mathbf{H}_m^T / N_f. \quad (13)$$

- MF (a.k.a. Rake) Receiver

$$\mathbf{G}_m^{\mathrm{MF}} := \mathrm{diag}\left(\mathbf{C}_m^T, \ldots, \mathbf{C}_m^T\right) \mathbf{H}_m^T / N_f. \quad (14)$$

- MMSE Receiver

$$\mathbf{G}_m^{\mathrm{MMSE}} := \boldsymbol{\Gamma}_m \mathbf{H}_m^T \left[\boldsymbol{\Gamma}_{\boldsymbol{\eta}\boldsymbol{\eta}} + \mathbf{H}_m \mathbf{F} \mathbf{H}_m^T\right]^{-1} \quad (15)$$

where $\mathbf{F}$ is an $N_1 A \times N_1 A$ block matrix:

$$\mathbf{F} := \begin{pmatrix} \mathbf{F}_{0,0} & \cdots & \mathbf{F}_{0,A-1} \\ \vdots & \ldots & \vdots \\ \mathbf{F}_{A-1,0} & \cdots & \mathbf{F}_{A-1,A-1} \end{pmatrix} \quad (16)$$

with $N_1 \times N_1$ blocks given by: $\mathbf{F}_{p,q} := \sum_{k,\ell=0}^{N_c-1} \mathbf{C}_k \boldsymbol{\Gamma}_{p,k,q,\ell} \mathbf{C}_\ell^T$, where $\boldsymbol{\Gamma}_{p,k,q,\ell} := \mathrm{E}\left[\beta_p(\mathbf{s}_k)\, \beta_q^T(\mathbf{s}_\ell)\right]$ is $K \times K$. Matrix $\boldsymbol{\Gamma}_{\boldsymbol{\eta}\boldsymbol{\eta}} := \mathrm{E}[\boldsymbol{\eta}(i)\boldsymbol{\eta}^T(i)]$ is $N_{L_1} \times N_{L_1}$, and block matrix $\boldsymbol{\Gamma}_m$ is $KA \times N_1 A$:

$$\boldsymbol{\Gamma}_m := \begin{pmatrix} \boldsymbol{\Gamma}_{m,0,0} & \cdots & \boldsymbol{\Gamma}_{m,0,A-1} \\ \vdots & \ldots & \vdots \\ \boldsymbol{\Gamma}_{m,A-1,0} & \cdots & \boldsymbol{\Gamma}_{m,A-1,A-1} \end{pmatrix} \quad (17)$$

with $K \times N_1$ blocks given by: $\boldsymbol{\Gamma}_{m,p,q} := \sum_{\mu=0}^{N_c-1} \boldsymbol{\Gamma}_{p,m,q,\mu} \mathbf{C}_\mu^T$.

Due to its structure, matrix $\mathbf{H}_m$ in (10) is not guaranteed to be full rank and therefore the ZF receiver (13) might not always exist (unlike the SISO model in [3]). When it is full rank, the output of the ZF receiver is equal to $\boldsymbol{\beta}_{s_m} + \mathbf{G}_m^{\mathrm{ZF}} \boldsymbol{\eta}$ which shows that MUI is suppressed and then leads to (almost) error-free symbol recovery in the noise-free (high SNR) case.

Therefore, assuming that the noise $\eta(t)$ is Gaussian, the optimal detector in the ML sense is given by:

$$\widehat{\mathbf{s}}_m(i) = \arg\min_{\mathbf{s}} \|\widehat{\boldsymbol{\beta}}_{\mathbf{s}_m(i)} - \boldsymbol{\beta}_{\mathbf{s}}\|^2_{\boldsymbol{\Sigma}^{-1}} \quad (18)$$

where $\boldsymbol{\Sigma} := \mathrm{E}[\breve{\boldsymbol{\eta}}(i)\breve{\boldsymbol{\eta}}^T(i)] = \mathbf{G}_m \boldsymbol{\Gamma}_{\boldsymbol{\eta}\boldsymbol{\eta}} \mathbf{G}_m^T$ is the correlation matrix of the filtered noise $\breve{\boldsymbol{\eta}}(i)$. Although this detector is optimal only for the ZF receiver, it will be used also for the other receivers (MF and MMSE).

5. PERFORMANCE

We first present a simulation example of the proposed downlink receivers in a frequency selective multipath environment and then derive an upper bound on the SER for the ZF receiver which is compared to the simulated perfromance.

5.1. Simulation Results

We present here simulations to illustrate the behavior of the different receivers for a given propagation channel and a set of parameters. The selected configuration is: a binary PPM modulation ($m = 1$), 4 users ($N_c = 4$), 2 symbols per burst ($K = 2$) and one frame ($N_f = 1$). Following [7] we have chosen: a frame duration $T_f = 100$ ns and a maximum delay spread equal

to 100 ns, hence a the chip duration $T_c = T_f/N_c = 25$ ns and a channel length $L_1 = 4$. Assuming the same guard time for the uplink and the downlink, we deduce that the bit rate is $D = mK/(2(N_1 + L_1)T_c) = 3.33$ Mbit/s.

The channel is modeled with 400 paths equally spaced in time within the maximum delay spread. The amplitude of each path is taken as a Gaussian variable and is linearly weighted to decrease to zero at the maximum delay spread (see *e.g.*, Fig. 9 in [7]). Thus, the continuous channel is given by:

$$h_{m,a,b}(t) = \sum_{k=0}^{399} c_k r_w(t + \tau_b - \tau_a - kT_p)(1 - k/400) \quad (19)$$

where $T_p = 0.25$ ns, c_k are independent zero mean Gaussian variables and $r_w(t)$ is the autocorrelation of the pulse shape function $w(t)$. In the PPM-IRMA system the received signal is the second derivative of the Gaussian function $\sqrt{\tau^3/3}(2/\pi)^{1/4}\exp(-t^2/\tau^2)$ (normalized to have $r_w(0) = 1$); hence, we have $r_w(t) = \exp(-t^2/(2\tau^2))[1-2(t/\tau)^2+(t/\tau)^4/3]$ where the parameter $\tau = .1225$ ns is adjusted to have a pulse width equal to 0.7 ns (see *e.g.*, [8]). Fig. 4 shows a realization of the channel $h_{m,0,0}(t)$ defined in (19).

Fig. 5 depicts the SER for the three receivers for one channel realization. We see that the rake performs poorly and exhibits a BER floor when the SNR goes to infinity. The MMSE performs the best while the ZF remains close to the MMSE.

5.2. Symbol Error Rate Bound for the ZF Receiver

Because the linear stage of the ZF receiver cancels the effect of the channel and therefore the MUI, we can derive an upper bound for the SER. Provided that the matrix $\mathbf{H}_m$ is invertible in (11), the output of the linear filter (13) can be expressed as: $\widehat{\boldsymbol{\beta}}_{s_m} = \boldsymbol{\beta}_{s_m} + \mathbf{G}_m^{\mathrm{ZF}}\boldsymbol{\eta}$. Then, given the symbol $\mathbf{s}_m$, the error probability for the ML detector is given by:

$$\mathrm{P}_e(\mathbf{s}_m) = \Pr\left\{\bigcup_{\mathbf{s}\in\mathcal{D}_\mathbf{s}\setminus\mathbf{s}_m} \boldsymbol{\delta}_\mathbf{s}^T\boldsymbol{\Sigma}^{-1}\boldsymbol{\delta}_\mathbf{s} + 2\boldsymbol{\eta}^T(\mathbf{G}_m^{\mathrm{ZF}})^T\boldsymbol{\Sigma}^{-1}\boldsymbol{\delta}_\mathbf{s} < 0\right\}$$

where $\mathcal{D}_\mathbf{s}$ is the set of all possible symbol vectors $\mathbf{s}$, and $\boldsymbol{\delta}_\mathbf{s} = \widehat{\boldsymbol{\beta}}_{\mathbf{s}_m} - \boldsymbol{\beta}_\mathbf{s}$. Introducing the notation: $d_\mathbf{s} = \boldsymbol{\delta}_\mathbf{s}^T\boldsymbol{\Sigma}^{-1}\boldsymbol{\delta}_\mathbf{s}$ and $\mathbf{v}_\mathbf{s} = 2(\mathbf{G}_m^{\mathrm{ZF}})^T\boldsymbol{\Sigma}^{-1}\boldsymbol{\delta}_\mathbf{s}$, the probability of error can be approximated using the *union bound* by:

$$\mathrm{P}_e(\mathbf{s}_m) \le \sum_{\mathbf{s}\in\mathcal{D}_\mathbf{s}\setminus\mathbf{s}_m} \Pr\left\{d_\mathbf{s}(\mathbf{s}_m) + \boldsymbol{\eta}^T\mathbf{v}_\mathbf{s} < 0\right\}, \quad (20)$$

where $d_\mathbf{s}(\mathbf{s}_m)$ is a constant and $\boldsymbol{\eta}^T\mathbf{v}_\mathbf{s}$ is a random Gaussian variable with zero mean and variance equal to $\sigma^2 = \mathbf{v}_\mathbf{s}^T\mathbf{v}_\mathbf{s}\sigma_\eta^2$, with $\sigma_\eta^2 = \mathrm{E}[\eta^2(n)]$; hence, we find $\Pr\left\{d_\mathbf{s}(\mathbf{s}_m) + \boldsymbol{\eta}^T\mathbf{v}_\mathbf{s}\right\} = \frac{1}{2}\mathrm{erfc}\left(d_\mathbf{s}(\mathbf{s}_m)/(\sqrt{2\mathbf{v}_\mathbf{s}^T\mathbf{v}_\mathbf{s}}\sigma_\eta)\right)$. Assuming that the symbols are equally probable, the SER for a given vector is equal to $p_K^A\,\mathrm{P}_e(\mathbf{s}_m)$ where $p_K^A = \frac{1}{A^K}\sum_{i=1}^K n_i\cdot(i/K)$ is the SER induced by a vector of length K with symbols drawn from an alphabet of size A and where n_i is the number of time i errors occur in this vector. We can show that $n_i = \binom{K}{i}(A-1)^i$ so that $p_K^A = \frac{A-1}{A}$ which is independent of K. Thus, we obtain:

$$\mathrm{SER}(\mathbf{s}_m) = \frac{A-1}{A}\cdot\mathrm{P}_e(\mathbf{s}_m), \quad (21)$$

from which, using (20), we deduce the following SER upper bound:

$$\mathrm{SER} \le \frac{A-1}{2A^{(K+1)}}\sum_{\mathbf{s}_i\in\mathcal{D}_\mathbf{s}}\sum_{\mathbf{s}\in\mathcal{D}_\mathbf{s}\setminus\mathbf{s}_i}\mathrm{erfc}\left(\frac{d_\mathbf{s}(\mathbf{s}_i)}{\sqrt{2\mathbf{v}_\mathbf{s}^T\mathbf{v}_\mathbf{s}}\sigma_\eta}\right). \quad (22)$$

Fig. 6 shows that for the same channel and parameters of Fig. 5, the SER of the ZF receiver and the bound given by (22) are very close.

6. REFERENCES

[1] S. S. Kolenchery, K. Townsend, and J. A. Freebersyser, "A novel impulse radio network for tactical wireless communications," *Proc. of the Milcom Conf.*, pp. 59–65, Bedford, MA, USA, Oct. 1998.

[2] C. J. Le Martret and G. B. Giannakis, "All-digital impulse radio with multiuser detection for wireless cellular systems," *IEEE Trans. on Communications*, May 2000, (submitted).

[3] C. J. Le Martret and G. B. Giannakis, "All-digital PPM impulse radio for multiple access through frequency-selective multipath," in *Proc. of Sensor Array and Multichannel Signal Proc. Work.*, Boston, March 2000.

[4] F. Ramirez-Mireles, M. Z. Win, and R. A. Scholtz, "Signal selection for the indoor wireless impulse radio channel," *Proc. of the 47th Vehicular Tech. Conf.*, pp. 2243–2247, Phoenix, AZ, USA, May 1997.

[5] R. A. Scholtz, "Multiple access with time-hopping impulse radio," in *Proc. of the Milcom Conf.*, Boston, MA, USA, Oct. 1993, pp. 447–450.

[6] S. Verdú, *Multiuser Detection*, Cambridge Press, 1998.

[7] M. Z. Win, X. Qiu, R. A. Scholtz, and V. O. K. Li, "ATM-based TH-SSMA network for multimedia PCS," *IEEE Journal on Selected Areas in Communications*, vol. 17, no. 5, pp. 824–836, May 1999.

[8] M. Z. Win and R. A. Scholtz, "Impulse radio: how it works," *IEEE Communications Letters*, vol. 2, no. 2, pp. 36–38, Feb. 1998.

[9] M. Z. Win and R. A. Scholtz, "On the robustness of ultra-wide bandwidth signals in dense multipath environments," *IEEE Communication Letters*, vol. 2, no. 9, pp. 51–53, Feb. 1998.

[10] P. II. Withington and L. W. Fullerton, "An impulse radio communications system," in *Proc. of the Intl. Conf. on Ultra-Wide Band, Short-Pulse Electromagnetics*, Brooklyn, NY, USA, Oct. 1992, pp. 113–120.

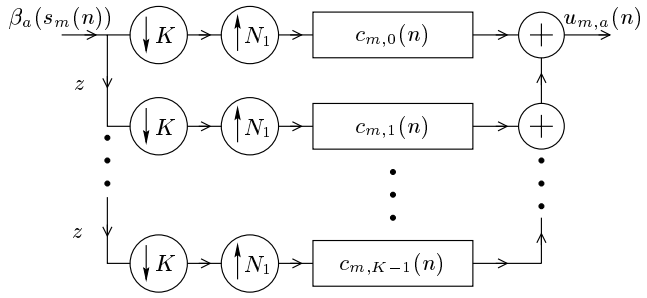

Figure 1: Filterbank implementation of the PPM-IRMA spreading for branch a ($N_1 = KN_fN_c$).

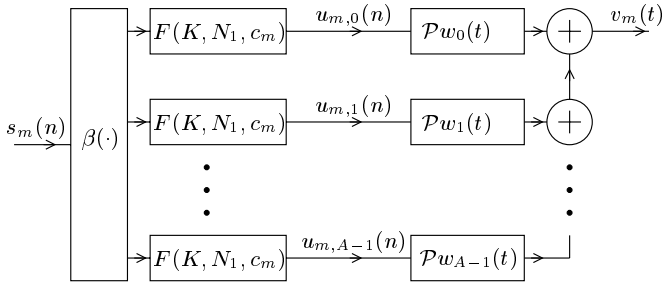

Figure 2: Continuous-time PPM-IRMA model (mth-user).

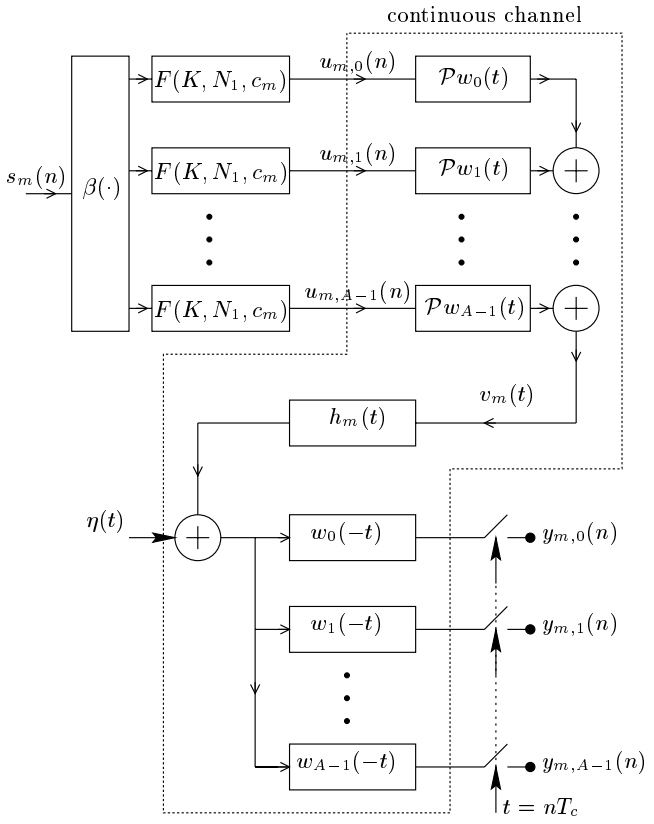

Figure 3: MIMO PPM-IRMA model (mth-user).

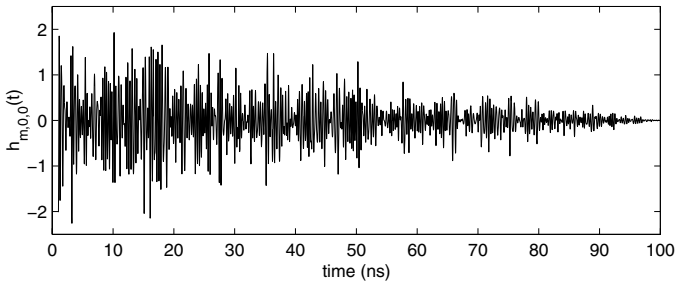

Figure 4: Example of channel impulse response for $h_{m,0,0}(t)$ using model in (19) with maximum delay spread equal to 100 ns.

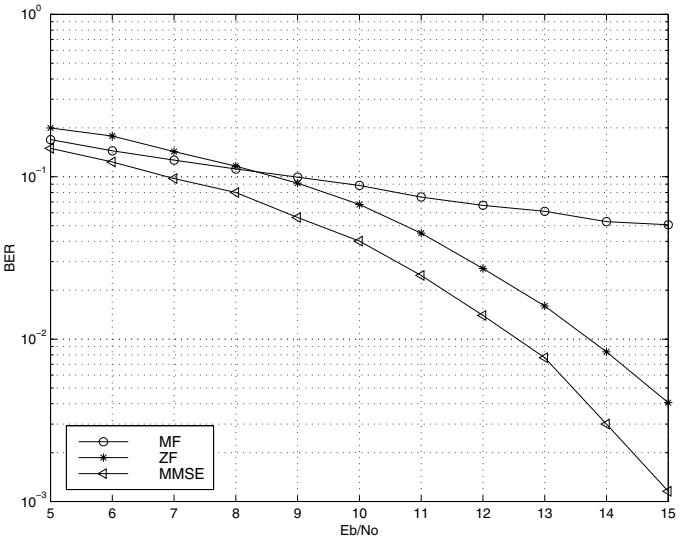

Figure 5: BER vs. E_b/N_0 for ZF, MMSE and MF receivers in the binary case using MIMO channel model in (19) and $K = 2$, $N_c = 4$, $N_f = 1$.

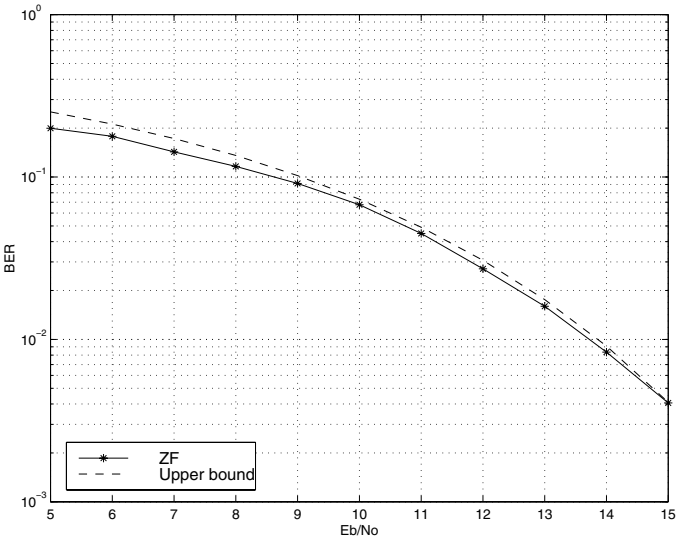

Figure 6: Comparing simulation vs. upper bound in (22) for the ZF receiver with the same parameters as in Fig. 5.

0-7803-6521-6/00/$10.00 (c) IEEE